LA-UR-01-2032
Approved for public release; distribution is unlimited.

Title: **Dislocations in Mo_5SiB_2 T2 Phase**

Author(s): R.D. Field, D.J. Thoma, J.C. Cooley, F. Chu, C.L. Fu, M.H. Yoo, W.L. Hults, and C.M. Cady

Submitted to:

http://lib-www.lanl.gov/la-pubs/00796391.pdf

Los Alamos National Laboratory, an affirmative action/equal opportunity employer, is operated by the University of California for the U.S. Department of Energy under contract W-7405-ENG-36. By acceptance of this article, the publisher recognizes that the U.S. Government retains a nonexclusive, royalty-free license to publish or reproduce the published form of this contribution, or to allow others to do so, for U.S. Government purposes. Los Alamos National Laboratory requests that the publisher identify this article as work performed under the auspices of the U.S. Department of Energy. Los Alamos National Laboratory strongly supports academic freedom and a researcher's right to publish; as an institution, however, the Laboratory does not endorse the viewpoint of a publication or guarantee its technical correctness.

FORM 836 (10/96)

Dislocations in Mo_5SiB_2 T2 Phase

R.D. Field[1*], D.J. Thoma[1], J.C. Cooley[1], F. Chu[1], C.L. Fu[2], M.H. Yoo[2], W.L. Hults[1], and C.M. Cady[1]

[1] Material Science and Technology Division, Los Alamos National Laboratory, MS G770, Los Alamos, NM, 87545, USA
[2] Metals and Ceramics Division, Oak Ridge National Laboratory, Oak Ridge, TN 37831-6114, USA
* corresponding author: (505) 667-5268 (fax), rdfield@lanl.gov

Abstract

Dislocation structures in a nearly single phase annealed Mo_5SiB_2 T2 alloy have been investigated by transmission electron microscopy (TEM). The dislocations have been subjected to Burgers vector and trace analyses to determine the slip directions and planes with the aid of image simulations generated using single crystal elastic constants derived from first principles calculations. The experimental results are compared to predicted slip directions and planes from anisotropic elasticity calculations. Thermal expansion coefficients have been measured by dilatometry and are compared to both calculated and previous experimental values measured using diffraction techniques. Lastly, preliminary compression testing has been performed on the single phase material at 1200°C.

Key words: Mo_5SiB_2 T2 phase, dislocations, Burgers vector, slip plane, CTE

1. Introduction

The T2 phase, which exhibits a distinct range of solubility around the Mo_5SiB_2 stoichiometry [1, 2], has received considerable attention recently as a potential constituent in Mo-Si based alloys for high temperature structural applications [3-5]. For example, the T2 phase has a high temperature stability limit (~2200°C) [2] and good oxidation resistance [6-8]. In a multi-phase alloy with a molybdenum matrix, the materials exhibit high-temperature creep strength [9,10] and room temperature flexure strength [11]. The interesting properties of the multi-phase alloys have prompted interest in the monolithic T2 phase properties. For example, recent results from room temperature Vickers indentation tests indicate that the hardness and the fracture toughness of the T2 phase are about 30% higher than those of the T1 phase [12]. The isotropic polycrystalline elastic properties indicate a stiff material with a higher Poisson ratio (0.26) than disilicides (0.18) [12]. These results, together with the nearly isotropic coefficient of thermal expansion (CTE) of the T2 phase [13], suggest that this phase has development potential as a structural material.

The T2 ternary intermetallic compound has a body-centered tetragonal Cr_5B_3 structure (I4/mcm), with lattice parameters of a=0.60nm and c=1.10nm. There are 32 atoms (20 Mo, 4 Si, 8 B) per unit cell in the Mo_5SiB_2 structure. This rather large unit cell raises the question of whether the T2 phase is deformable or can accommodate dislocations. It has been reported that numerous dislocations exist in nearly single phase Mo_5SiB_2 [12] and dislocations have also been observed in T2 constituents of multiphase alloys subjected to creep deformation [9, 10]. In this study, a more detailed investigation of the dislocations in annealed T2 phase material was performed in the transmission electron microscope (TEM). The dislocations and the potential for slip are analyzed in terms of the crystallographic structure of the intermetallic using anisotropic elasticity theory.

2. Experimental procedure

The material for this study was produced by arc-melting. The starting materials were solid 99.95% Mo and 99.9999% Si, and 99.995% submicron amorphous B powder. The boron was pelletized prior to melting to facilitate handling. The specimens were re-melted 8-10 times to ensure mixing. The masses of the initial charges were 40-45g and total mass loss after melting was 0.5-1.0%. Samples for TEM investigations were heat-treated at 1600°C for 336 hours in a high-purity, flowing argon environment.

Polycrystalline rods were made by arc-melting 7-10g of the above cast specimens on a hearth with a 5 mm diameter by 30 mm deep cylindrical hole drilled into the bottom. After melting the charge, a slight vacuum was pulled on the backside of the hole, allowing the molten alloy to flow into it. This resulted in a high solidification rate, minimizing elemental segregation. The resulting rods had some internal cracking, but were monolithic, suggesting that liquid undercooling did occur. Since x-ray diffraction showed the material to be >95% T2 phase, no annealing was performed on these specimens. These rods were cut into 5mm lengths by wire EDM for compression tests and dilatometry.

Slices for TEM specimens, ~0.5mm in thickness, were cut from the arc-melted and annealed buttons by wire EDM. These were then carefully ground to ~150μm thickness using 400 grit SiC paper for the initial grinding, followed by 600 grit SiC and ending with 9μm Al_2O_3 film. An abrasive core drill was used to remove 3mm discs, which were mechanically dimpled, initially using 6μm diamond paste, followed by 3μm diamond paste during the final stage. The specimens were ion milled to final thickness in a Gatan Precision Ion Polishing System (PIPS) instruments at an accelerating voltage of 4KV. TEM analysis of the dislocations was performed on a Philips CM30 instrument operating at 300KV.

CTE was measured using a MMC quench-deformation dilatometer. The 5 mm diameter by 5 mm long specimens were inductively heated (~1 MHz) to 1200°C with a heating and cooling rate of 0.4 K/s. The vacuum level was 10^{-5} torr.

The compressive properties of the materials were measured on a MTS model 810 hydraulic load frame equipped with a vacuum furnace. The samples were ramped to temperature at 25°C/min and held at temperature for 10 minutes prior to testing. The samples were tested at a strain rate of 0.001/s and deformed to ~ 20% strain or until the sample failed.

3. Experimental results

The TEM specimen was found to contain numerous single, unfaulted dislocations, along with occasional dislocation terminated stacking faults. A typical grain is shown in Figure 1. The cluster of dislocations in the right-center of the micrograph was subjected to detailed Burgers vector and line direction analyses. The faulted dislocations were not analyzed and will be the subject of a future investigation.

Figure 2 is a weak beam micrograph of the cluster of dislocations investigated. The widths of the dislocation images are ~4nm; no dissociation could be detected in the micrographs. Selected micrographs from the Burgers vector analysis are shown in Figure 3. It is apparent from these

micrographs that there are three different Burgers vectors represented in this cluster. The curved dislocation is out-of-contrast for the (600), (20~4), and (40~4) **g**-vectors, indicating a Burgers vector parallel to [010]. Five of the six straight dislocations are clearly out-of-contrast for the (21~1), (330), and (121), **g**-vectors, indicating a Burgers vector parallel to [~11~1]. This Burgers vector also would result in an out-of-contract condition for the (40~4) **g**-vector, which is less clear from the micrograph. The sixth straight dislocation (bottom of the micrographs) did not yield sufficient data for an unambiguous Burgers vector determination. The magnitudes of the Burgers vectors can be deduced from the body-centered tetragonal crystal structure, yielding [010] and 1/2[~11~1], respectively.

Line direction analyses were performed on the [010] dislocation and the center 1/2[~11~1] dislocation (the other four 1/2[~11~1] dislocations appear to be parallel to the center one). For the curved dislocation, the line direction analysis was performed on the line connecting the endpoints (i.e. intersections with the foil surfaces). This was determined to be approximately [1~10], indicating that the dislocation is lying on a (001) plane. This is consistent with observations that the curvature of the dislocation was maximum near the [001] zone axis and decreased with increasing tilt away from this direction. The 1/2[~11~1] dislocation has a line direction near [14 7 3], indicating that it is lying on a (~~112) plane.

To aid in the Burgers vector analysis, dislocation image simulations were performed using the Tetdis program of Head et al. [14]. Since experimentally measured elastic constants for this phase were not available, calculated values were used (Table 1). Comparisons between experimental and simulated images for in-contrast and out-of-contrast conditions are provided in Figure 4. There is very good agreement between the experimental and simulated images. Of particular interest is the image for the (40~4) **g**-vector, for which the unusual residual contrast observed experimentally is predicted by the simulation.

Compression tests were performed at 1200°C on the 5 mm diameter by 5 mm long samples. Internal cracks were present in the as-machined specimens and evidence of extensive cracking during testing was observed in the stress-strain curves. No evidence of plastic yielding was observed. Maximum nominal loads of 700MPa were recorded during one of the tests, even with numerous cracks in the specimens. Thus, the yield stress of the T2 phase at 1200°C is well in excess of 700MPa.

Results from the CTE measurements in the temperature range from RT to 1200°C are presented in Figure 5. The average CTE is 8.2×10^{-6}/°C. This value is in good agreement with calculated values (7 to 8 $\times 10^{-6}$/°C [13]) and data obtained from diffraction techniques (neutron: 7.5 and 7.9×10^{-6}/°C [15], syncrotron x-ray: 7.2 and 7.7×10^{-6}/°C [16]; values for the c and a axes, respectively) in this temperature range.

4. Possible Slip Systems Based on the Anisotropic Elasticity Theory

In this section, we examine possible slip systems in the T2 phase by calculating energetic and kinetic factors for dislocation formation and mobility based on the crystallography and calculated elastic constants.

The calculated lattice parameters and second-order elastic constants are listed in Table 1. These calculations were performed using the full-potential linearized augmented plane-wave method within

the local-density-functional approach. For the determination of elastic constants, the lattice is deformed uniformly in six different ways, and for each of them we calculate the total energy as a function of strain (up to 2-3%; see Ref. [17] for details). The calculated elastic constants are in good agreement with a recent measurement for the T2 single phase by the resonance method [18]. The averaged elastic moduli (E = 384 GPa, B = 272GPa, and G = 152 GPa) are slightly higher than those of Mo_5Si_3, and are consistent with the measured values of a multi-phase T2 matrix (E = 361 GPa, B = 254 GPa, and G = 143 GPa) [12]. An additional examination of the accuracy of the calculations can be made by comparing calculated CTE values with experimental measurements. These calculations have been made [13], and the results are in good agreement with experimental values measured by diffraction techniques [15,16], and by dilatometry in the current study.

According to the anisotropic elasticity theory of dislocations, the line energy per unit length of a dislocation is [19]

$$E = \frac{Kb^2}{4\pi} \ln\left(\frac{R}{r_0}\right) \quad , \qquad (1)$$

where b is the magnitude of the Burgers vector, K is the energy factor which is a function of the elastic constants and the dislocation character, and R/r_0 is the ratio of the outer and inner cut-off radii of the elastic field around a dislocation. The stress required to surmount the lattice resistance to dislocation motion is called the Peierls stress and given by [19]

$$\sigma_p = 2K \exp\left(\frac{-2\pi\zeta}{b}\right) \quad . \qquad (2)$$

The exponent is proportional to the ease-of-gliding (EOG) parameter,

$$\frac{\zeta}{b} = \frac{1}{2}(KS)\frac{d}{b} \quad , \qquad (3)$$

which consists of an elastic anisotropy factor (K_eS_{66} and K_sS_{44} for the edge and screw character, respectively) and a geometrical factor, d/b, where S_{ij}'s are the reduced elastic compliance constants referred to the dislocation coordinate axes and d is the interplanar spacing for a given slip system.

Table 2 shows the calculated results of the dislocation line energies (E*) and the EOG parameters (ζ/b) for some potential slip systems with low index (hkl) slip planes in the T2 phase. The logarithmic factor is kept as $R/r_0 = \exp(4\pi)$, such that the dislocation line energy is simply given by the prelogarithmic factor, i.e., $E^* = Kb^2$. The line energy is the lowest for (010)[100] slip and the EOG parameter is the largest for (011)[100] slip. With the next smallest Burgers vector of 1/2[111], the (11~2) slip plane is favored over the (1~10) plane for both the E* and ζ/b parameters. The line energies for [110] and [001] Burgers vectors are about a factor of two higher than those of [100] and 1/2[111].

The energy factors for screw dislocations with Burgers vectors of [100], 1/2[111], [110], and [001] are K_s = 151, 148, 172, and 179 GPa, respectively, which may be compared with the isotropic value (Hill's average) of G = 152 GPa. For [100] and 1/2[111] slip vectors, the ratios of K_e/K_s and

K_eS_{66}/K_sS_{44} are both in the range of 1.31-1.43. This suggests that energetically the screw component is more favored, but the edge component would be relatively more glissile with the same factor in the range of 31-43%.

5. Discussion

The two shortest lattice translation vectors for this compound are <100> (0.600nm) and 1/2<111> (0.696nm). In previous investigations of crept specimens containing the T2 phase (in addition to Mo_3Si and Mo_5Si_3 (T1) phases), dislocations with <100> [9, 10] and <110> [9] Burgers vectors were tentatively identified. However, the Burgers vector analysis results for the latter were cited as "not definitive" by the authors, since only a single out-of-contrast condition was observed. The calculations in Section 4 predict <100>/{010} and 1/2<111>/{112} as the most likely to be active in this material. This is largely consistent with the experimental results of the current investigation, although the slip plane observed for the <100> Burgers vector in this study was found to be {001}, rather than {010}. This slip plane is consistent with the previous experimental results on crept multiphase specimens, however [9].

It is believed that the dislocations observed in the current investigation had moved in response to thermal stresses generated during cooling. However, since the material was not intentionally strained, there is no guarantee that the observed dislocations were indeed actively slipping. At the very least, these dislocations represent the Burgers vectors available in the microstructure for deformation. Dislocation studies in intentionally deformed specimens are planned. The analysis in Section 4 is based on the crystallographic and elastic properties of perfect dislocations only. A more complete analysis of slip behavior will require atomistic modeling. Future analyses will also include the possibility of the dissociation of dislocations into partial dislocations bounding a strip of stacking fault. While no dissociation of the dislocations was observed within the resolution dictated by widths of the dislocation images (~4nm), the possibility of a dissociation smaller than this is, of course, not precluded by these observations.

The high integrity of the T2 phase in multiphase alloys is difficult to reproduce in single phase material. The single phase T2 specimens produced in this study contain numerous internal cracks. This is a major obstacle in performing deformation studies of this material. Investigations of T2 deformation in multiphase materials is therefore a more expedient approach. However, high integrity single phase material is necessary for fundamental studies of slip system activation, particularly measurements of critical resolved shear stresses. Therefore, deformation studies of both multiphase and single phase alloys are planned in the future.

6. Conclusions

Dislocations in annealed Mo_5Si_3 T2 phase were investigated in the TEM. Two types of dislocations were analyzed and the following slip systems identified: <100>/{001} and 1/2<111>/{112}. The slip directions are consistent with the two smallest lattice translation vectors in the T2 crystal structure and agree with those predicted by theoretical calculations. The {112} slip plane for the <111> Burgers vector is also in agreement with these calculations. The predicted slip plane for the <100> Burgers vector is {010}, rather than the {001} plane observed here. However, the observed slip plane is consistent with previous experimental observations on crept specimens. Additional studies of active slip systems in intentionally deformed material are planned.

Acknowledgements

This research was sponsored by the Division of Materials Sciences and Engineering, Office of Basic Energy Sciences, U. S. Department of Energy, under DE-AC05-00OR22725 with UT-Battelle, LLC.

References

1. Nowotny H, Dimakopoulou E, Kudielka H. Monatsh. Chem. 1957;88:180.
2. Nunes CA, Sakidja R, Dong Z, Perepezko JH. Intermetallics 2000;8:327.
3. Berczik DM. Method for enhancing the oxidation resistance of a molybdenum alloy, and a method of making a molybdenum alloy, 1997. United States Patent No. 5,595,616.
4. Berczik DM. Oxidation resistant molybdenum alloy, 1997. United States Patent No. 5,693,156.
5. Meyer MK, Kramer MJ, Akinc M. Adv. Mater. 1996;8:85.
6. Meyer MK, Akinc M. J. Am. Ceram. Soc. 1996;79:938.
7. Meyer MK, Akinc M. J. Am. Ceram. Soc. 1996;79:2763.
8. Meyer MK, Thom AJ, Akinc M. Intermetallics 1999;7:153.
9. Meyer MK, Kramer MJ, Akinc M. Intermetallics 1996;4:273.
10. Nieh TG, Wang JG, Liu CT. Intermetallics 2001;9:73.
11. Schneibel JH, Liu CT, Easton DS, Carmichael CA. Mater. Sci. Eng. 1999;A261:78.
12. Chu F, Thoma DJ, McClellan KJ, Peralta P, Fodran E. In: High-Temperature Ordered Intermetallic Alloys VIII. MRS Symp Proc 1999;552:KK6.7.1 .
13. Fu CL, Wang X. Philos. Mag. Lett. 2000;80:683.
14. Head AK, Humble P, Clarebrough LM, Morton AJ, Forwood CT. Computed Electron Micrographs and Defect Identification. North Holland Publishing Company, Amsterdam, The Netherlands:1973.
15. Rawn CJ, Schneibel JH, Hoffmann CM, Hubbard CR. Intermetallics 2001;9:209.
16. Zhao H-L, Kramer M, Akinc M, Kycia S, Margulies L, Haeffner D. Presented at the MRS Fall Meeting, Boston, MA, Nov. 2000.
17. Fu CL, Wang X, Ye YY, Ho KM. Intermetallics 1999;7:179.
18. Ito K, Ihara K, Tanaka K, Fujikura M, Yamaguchi M. Intermetallics 2001;9:591.
19. Hirth JP, Lothe J. Theory of Dislocations. McGraw-Hill Publishing Co., New York, NY:1982.

Table1. Calculated lattice parameters and elastic constants of Mo_5SiB_2

a (Å)	c (Å)	C_{11} (GPa)	C_{12} (GPa)	C_{13} (GPa)	C_{33} (GPa)	C_{44} (GPa)	C_{66} (GPa)
6.03	11.0	483	154	188	419	179	127

Table 2. Elastic line energy and the ease-of-gliding parameter for possible slip systems (edge dislocations) in Mo_5SiB_2

b	(hkl)	K_e (GPa)	E* (nJ/m)	K_eS_{66}	ζ/b
[100]	(002)	214	77.7	1.19	0.545
[100]	(020)	198	72.1	1.56	0.391
[100]	(011)	205	74.3	1.50	0.659
1/2[111]	(1~10)	203	98.5	1.22	0.375
1/2[111]	(11~2)	199	96.1	1.60	0.386
1/2[111]	(12~3)	199	96.5	1.57	0.244

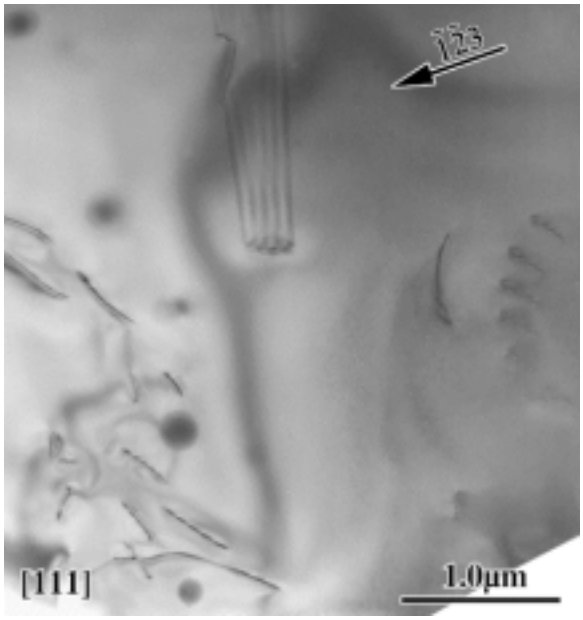

Figure 1. Low magnification TEM micrograph of cast and heat treated Mo_5SiB_2 phase showing perfect dislocations and stacking fault.

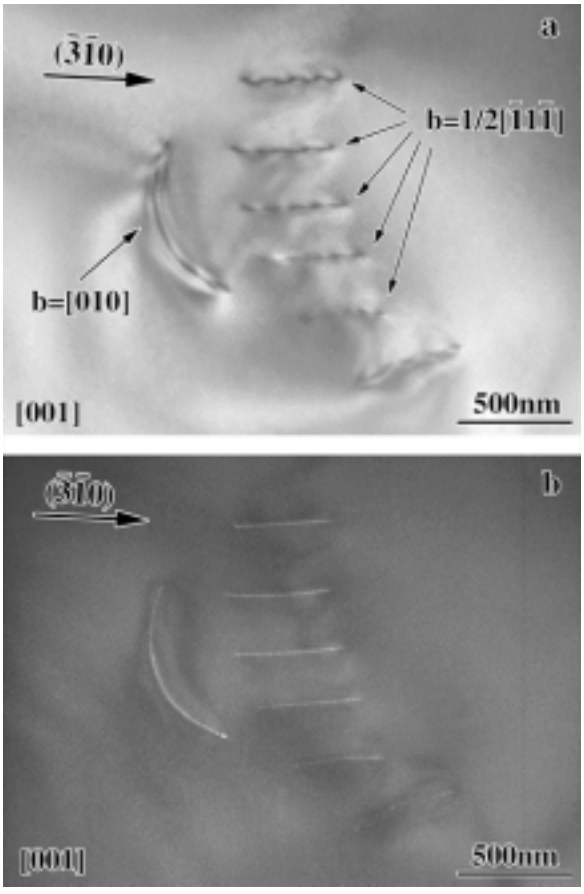

Figure 2. Weak beam TEM micrograph of analyzed dislocations (from right side of micrograph in Figure 1).

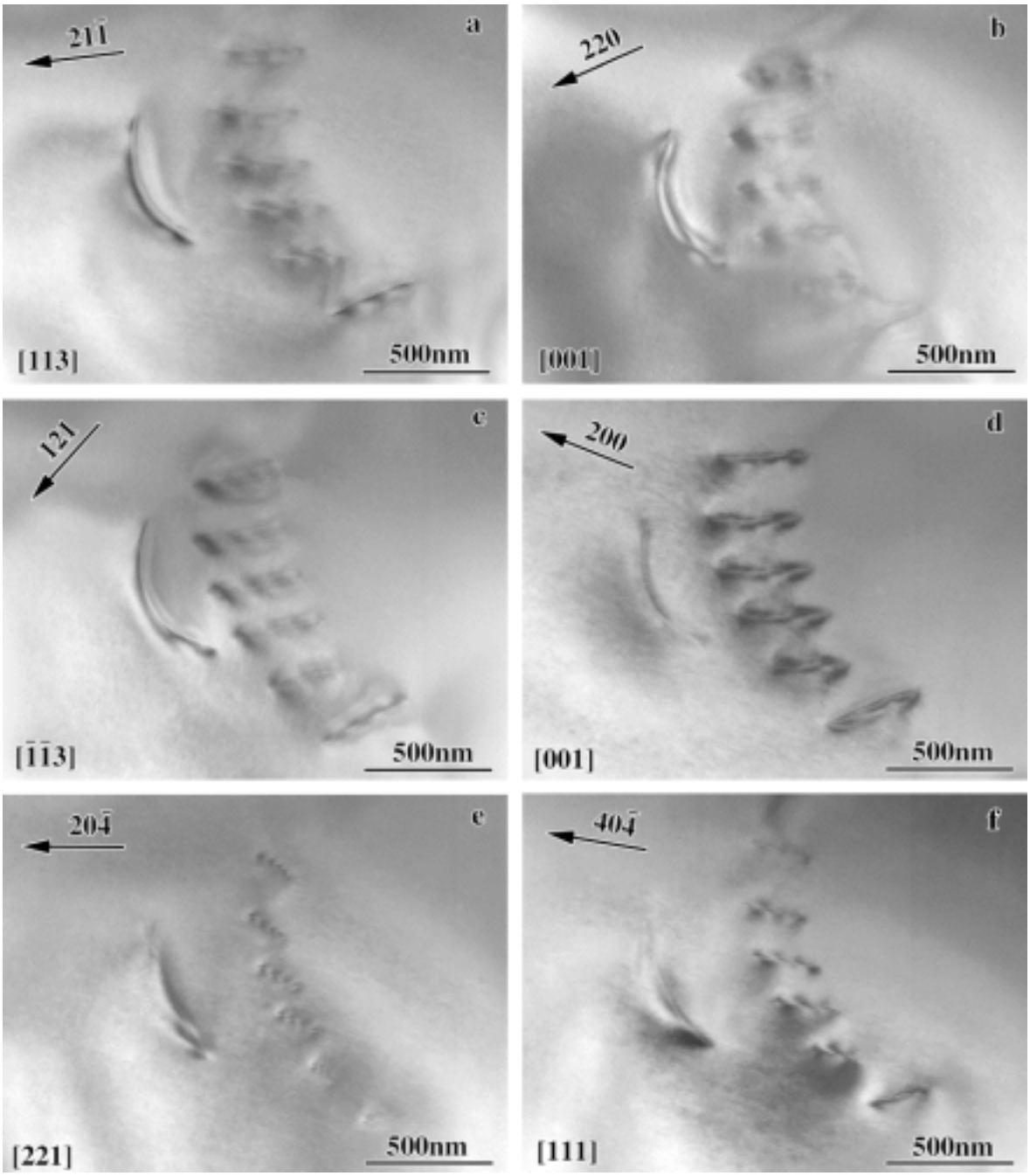

Figure 3. Bright field TEM micrographs used for Burgers vector and trace analyses of dislocations shown in Figure 2.

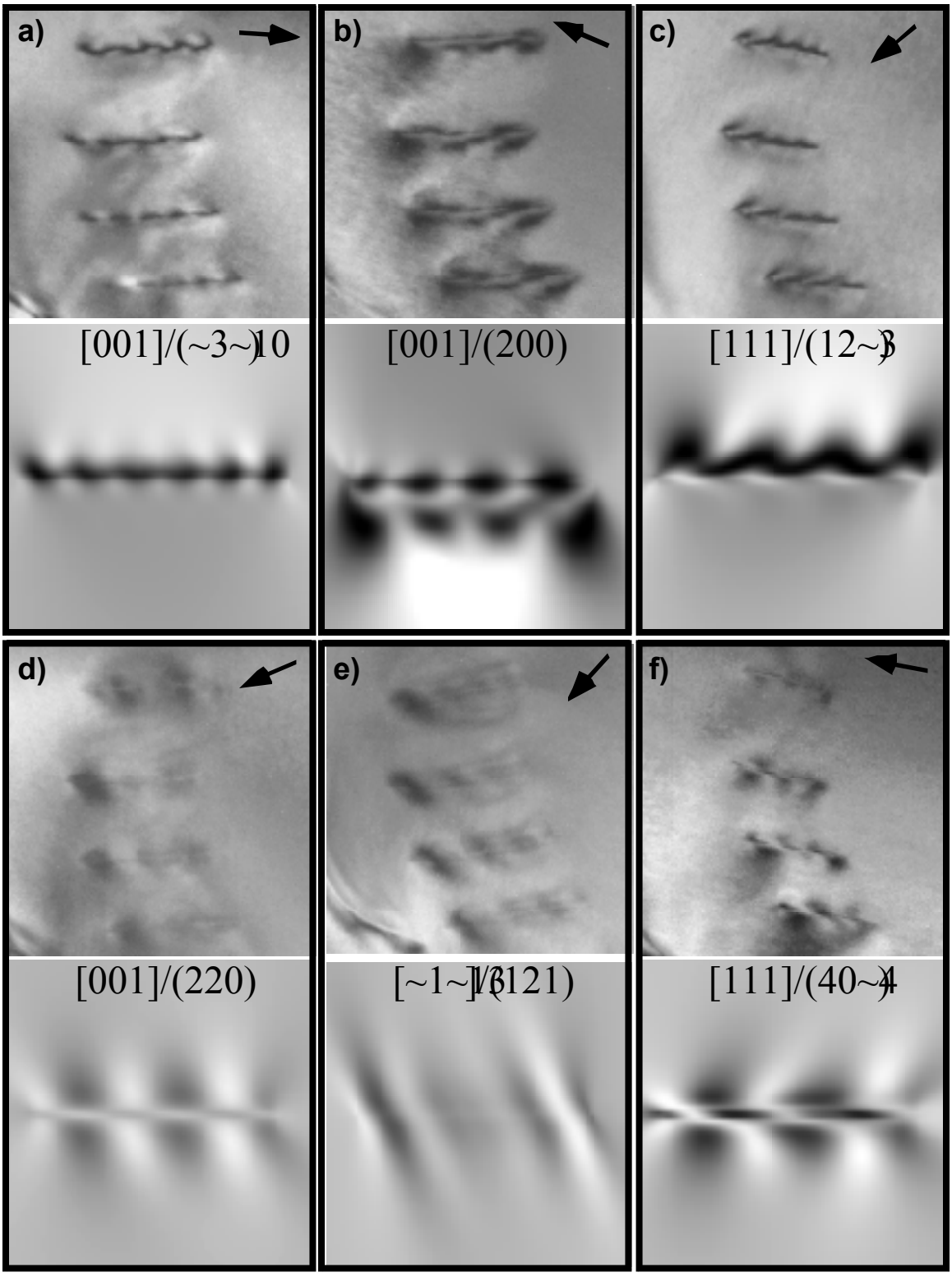

Figure 4. TEM experimental (top) and simulated (bottom) images of **b**=1/2[~11~1] dislocations for six different conditions. a-c are in-contrast images, d-f are out-of-contrast. Beam directions and **g**-vectors are provided on the simulated images; arrows on experimental

images indicate directions of **g**-vectors. (**g**-vectors given as reflecting planes in real space and are therefore surrounded by "()")

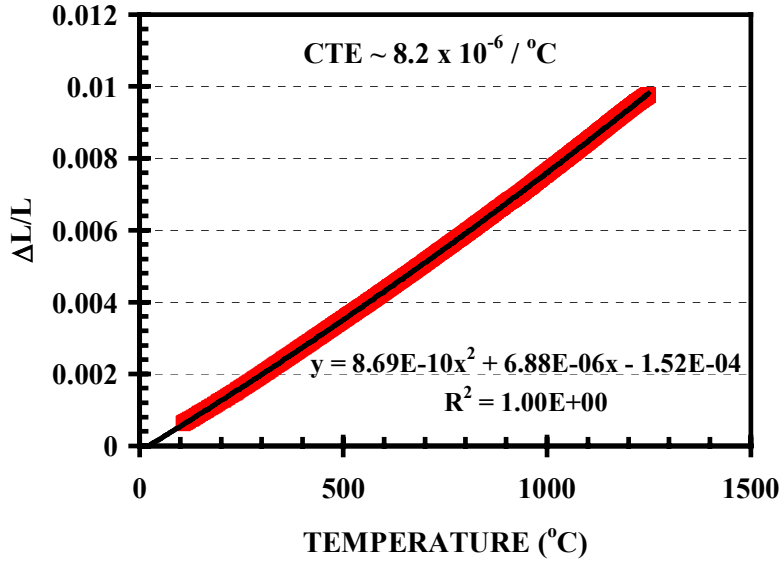

Figure 5. Plot of dilatometery data from Mo_5SiB_2 phase specimen with average CTE value for this temperature range.